NTU Journal for Renewable Energy (2026) Vol. 10 (1): 66-77
DOI: https://doi.org/10.56286/chgqph77

IRAQI Academic Scientific Journals

ISSN: 2788-9912 (print); 2788-9920 (online)
NTU Journal for Renewable Energy
Available online at:
https://journals.ntu.edu.iq/index.php/NTU-JRE

Improving the Mechanical Properties of Wind Turbine Blades Using Hybrid Composite Materials

Khuder N. Abed[1], Marwa Kh. Rashid[2], Mohammed W. Muayad[3], Afrah T. Awad[4]

[1]Department of Mechanical Engineering, College of Engineering, University of Diyala, Diyala, Iraq

[2,3,4] Renewable Energy Research Centre - Kirkuk, Northern Technical University, Kirkuk, Iraq

Article Informations

Received: 29 – 12 – 2025
Received in Revised form: 25-02-2026
Accepted: 08 – 03 - 2026
Published: 16 – 03 – 2026

Corresponding Author:
Afrah T. Awad

Email:
afrah.turki@ntu.edu.iq

Key words:
Kevlar-reinforced hybrid composite ; wind turbine blades; mechanical properties; wear behavior ;Wind Turbine ;Hybrid Composite Materials

ABSTRACT

This study investigates the enhancement of mechanical properties of wind turbine blade materials using Kevlar 49 fiber–reinforced epoxy hybrid composites. Three samples were fabricated using a hand lay-up technique with various configurations: Sample 1 (Kevlar fibers and epoxy), Sample 2 (Kevlar fibers, epoxy, and iron powder), and Sample 3 (Kevlar fibers, epoxy, graphite, and iron powder). All samples were cut and machined in accordance with ASTM D3039 and ASTM G65. The three samples were then subjected to Wear, hardness, and tensile tests to verify their performance. The results showed that Sample 2 had the highest hardness (70 Vickers), indicating high resistance to deformation. Meanwhile, Sample 1 exhibited the lowest wear rate ($< 3.093 \times 10^{-8}$ g/cm³), indicating high wear resistance. During tensile testing, sample 1 achieved the highest strength in both 90° (139.42 MPa) and 45° (237.5 MPa) fiber directions, with corresponding maximum loads of 2.9 kN and 5.7% strain at failure in the 45° orientation. Adding iron and graphite powders had a minimal effect on mechanical performance. Overall, Sample 1 demonstrated the most balanced mechanical response, with comparable hardness, wear resistance, and tensile strength among the investigated materials.

Introduction

The most important structural components under loading during the life cycle of a complete wind farm are the wind turbine blades, and the mechanical performance has an impact on operational efficiency, lifetime, and operational reliability. Since larger capacity wind turbines are constantly being developed, the materials used must have better specific strengths than ever before and also possess characteristics that make them resistant against fatigue, abrasion and other performance degradation under alternating dynamic loads. These demands have led to, and continue to lead to even greater development of composite materials for wind turbine blade use.

Hybrid composite materials, polymer matrix composites reinforced with fibres and enhanced by particulate or nanoscale additives, have attracted interest for their use in renewable energy and structural engineering. These systems enable tuning mechanical properties by combining multiple reinforcement mechanisms within a single composition. It is known from the literature that polymer or fiber-reinforced composites may be reinforced with micro- and/or nanoscale materials[1-5] fillers, for these cases they make for better hardness, tensile strength, wear resistance and durability compared to un filled compounds in order to obtain good performance at high structural application. [6],[7].

Apart from materials, rotor configuration and blade design also play a role on wind turbine blade performance. The Darrius type of vertical-axis wind turbine (VAWT) has been widely researched because its aerodynamic and dynamic behaviors change under loads [8]. Such considerations result in complex stress states in blade structures and emphasize their reliance on mechanically strong materials.

Significant efforts were devoted to the mechanical behavior of hybrid composites, particularly with respect to erosion resistance, fatigue strength and damage tolerance. The use of hybrid reinforcement to enhance the erosion resistance and fatigue behavior has also been successfully applied on rotor blade and aerospace applications [9–11]. Further studies on kenaf-, Kevlar- and glass fiber-reinforced hybrid composites have shown prospects in fatigue behavior, energy absorption, and structural service life [12–17]. Composites are still critical material in aerospace and high engineering fields to demonstrate superior mechanical properties and ability to deal with harsh service conditions [18–21], particularly the advanced load carrying potential of composites, as well as health monitoring impact on long-term reliability have been highlighted in recent review articles[22],[23].

The composites with Kevlar garner great interest because of the high tensile strength, toughness and good fatigue performance. The experimental study results have also shown that the Kevlar-reinforced composites can improve impact resistance and damage tolerance of wind turbine blade structures significantly [24]. This is, for example, achieved by hybridizing Kevlar with glass or carbon fibres and also advanced carbon-based fillers to improve stiffness, strength and mechanical stability [25],[26]. Structural mass and Long-term reliability of large wind turbines using carbon fibre composites have been reported to come down as well.[27].

Despite these advances, limited experimental studies have systematically investigated the combined effects of Kevlar 49 fibre reinforcement and particulate fillers, such as iron and graphite powders, on the mechanical behavior of wind turbine blade materials. In particular, the influence of these fillers on hardness, wear resistance, and tensile performance under off-axis loading conditions remains insufficiently explored.

Therefore, the objective of this research work is to fabricate and evaluate Kevlar 49 fibre–reinforced epoxy hybrid composites for wind turbine blade applications. Experimental results regarding the hardness, wear performance, and tensile failure strength at fibre orientations of 90° and 45° of iron powder and combined iron–graphite–filled Kevlar/epoxy are compared with unmodified Kevlar/epoxy composite, shedding light on their feasibility for wind turbine blade structures.

1. Methodology

Based on previously published studies [21–26], Kevlar fibres (Kevlar 49), Sikadur-52 epoxy resin, and selected particulate fillers, namely iron powder and graphite, were chosen for the fabrication of the hybrid composite systems investigated in this study. These materials were selected due to their well-established influence on the mechanical performance of fibre-reinforced composites.Kevlar fibres are known to enhance tensile strength and fatigue resistance in laminated structures [21-23], while epoxy matrices provide effective fibre–matrix interfacial bonding and good resistance to environmental ageing [23,24]. In addition, iron powder has been reported to improve hardness and wear resistance [21,28], whereas graphite fillers enhance tribological performance due to their lubricating properties [11,14].

In the present work, these materials were combined using a tailored fabrication approach to produce Kevlar-49-reinforced hybrid composites suitable for wind turbine blade applications, addressing specific mechanical performance requirements identified in previous studies.

1.1 Criteria for Selecting Operating Parameters and Material Combinations

In this study, five main criteria were used when selecting operating parameters and material combinations:

1. The combinations were chosen to attain optimal tensile strength, stiffness, and wear resistance during wind turbine blade operation.
2. Ensuring a strong bond between the Kevlar 49 fibers, Sikadur-52 epoxy resin, and fillers to sustain structural stability.
3. Optimizing the weight-to-power ratio to improve blade efficiency without excessive weight increase.
4. Using fillers (such as iron powder and graphite) that have proven effective in enhancing stiffness, tribological properties, and impact resistance in composite materials.
5. Selecting materials that are readily available, affordable, and suitable for manual assembly and hardening processes.

1.2 Error Bar Variability Control

In Figures 8,9 and 11, differences in error bars can alter the interpretation of material performance across testing parameters. To minimize these effects, all tests were performed at least three times under similar environmental conditions (temperature: 23 ± 1 °C; relative humidity: 50 ± 2%) using the same calibrated equipment and test methods. Outliers were removed per ASTM E178-16, and average values were taken with standard deviations. This method helped minimize the impact of experimental variation on the comparative results, thereby increasing the reliability of assessments for material hardness, abrasion resistance, and tensile strength.

1.3 Kevlar 49 fiber

Kevlar 49 reinforces the leading edge of wind turbine blades, which are prone to fatigue damage. By strengthening this area with Kevlar 49, the blades become more durable and fatigue-resistant, thereby reducing the risk of failure. Kevlar fiber is chosen as the reinforcing material for the matrix due to its advantages, including high strength, toughness, thermal stability, lightweight, and cost-effectiveness. Table 1 presents the properties of Kevlar 49 fiber.

This section presents the complete modelling, control system design, and simulation setup for the proposed hybrid Artificial Neural Network–Proportional Integral Derivative (ANN-PID) speed control of a Permanent Magnet Synchronous Motor (PMSM). The methodology is organized into five main parts: mathematical modelling of the PMSM, conventional PID controller design, ANN-based controller development, hybrid ANN-PID control strategy, and simulation setup. The complete simulation model for the designed system is shown in Figure (2)

Table 1. Kevlar 49 Material Properties [21]

Mechanical Properties	Value
Tensile Strength, Ultimate	3000 MPa
Elongation at Break	2.4%
Tensile Modulus	112 GPa
Tenacity	2.08 N/tex
Poisson's Ratio	0.36
Specific Heat Capacity	1.42 J/g °C
Thermal Conductivity	0.0400 W/m-K
Maximum Service Temperature, Air	149-177 °C
Shrinkage	<= 0.100%

The optimal method, which involves carefully embedding layers of Kevlar 49 fiber (4 cm × 2 cm), is employed to strengthen the leading edge of Kevlar-reinforced hybrid composite blades (the area most affected and prone to damage), thereby enhancing the fatigue resistance of the blade—figure (1): Construction of Kevlar 49 fiber with some insights.

Figure (1): Structural Composition of Kevlar 49 Fibre

1.4 Epoxy-type Sikadur-52

Epoxy (Sikadur-52) is produced by the company Sika Yapıkim Yaşallan A.Ş., Istanbul Deri Organize Sanayi Bölgesi, Türkiye. It is a fast-curing, water-resistant, chemically and UV-resistant, two-component injection resin. Its applications include structural bonding of steel elements and section beams, as well as concrete repair and protection against oxidation for chemical anchoring.

Combining Sikadur-52 epoxy with Kevlar 49 fiber, iron powder, and graphite powder to produce the hybrid composite yields superior properties. Sikadur-52 acts as a high-strength adhesive that effectively bonds these materials due to its high strength and toughness. Its excellent thermal stability ensures that the compound does not break down or off-gas during service, while its superior water and chemical resistance allow reliable performance in harsh conditions.

1.5 Iron powder

Iron powders are added to the hybrid composite to enhance tensile strength, impact toughness, and fatigue resistance, while also reducing weight. This, in combination, helps to make the blades stronger while allowing them to withstand higher fatigue loads. The fabrication processes for iron powder are broadly classified into two types: atomized iron powder production and reduced iron powder. The former is supplied for die-pressing products, whereas the latter, together with appropriate alloying elements, is applicable to electrical components or magnetic materials through sintering. Figure 2 shows the appearance of iron powder used as a strengthening element in composite materials.

Figure (2) Iron Powder as a Strength Enhancer in Composite Materials

1.6 Graphite powder

A hybrid composite made of Sikadur-52 epoxy, Kevlar 49 fiber, iron powder, and graphite powder offers enhanced mechanical properties. Graphite acts as a filler that contributes to enhancing the strength of the composite structure. This results in a material with significantly higher impact resistance, stiffness, and strength, making it suitable for demanding applications that require high mechanical durability. Figure 3 illustrates the graphite powder–reinforced composite. Additionally, Table 2 presents the mechanical properties of graphite powder [29].

Table 2: Mechanical Properties of Graphite Powder

Property	Value
Modulus of Elasticity	8-15 GPa
Compressive strength	20-200 MPa
Flexural strength	6.9-100 MPa
Shear strength	10-15 MPa
Hardness (Mohs)	1.0-2.0
Poisson's ratio	0.25-0.30

Figure (3) Graphite Powder Reinforcing Composite

2.7 Preparation of Composites:

The composite material preparation method involved a sequential process to create the composite samples. The following steps were taken:

1. Step one consisted of preparing the aluminum molds by cleaning and coating them with a barrier layer to inhibit composite material adhesion. And the dimensions of the molds were verified against ASTM D3039 and ASTMG65 (tensile test and wear test, respectively). It was to make sure that all of the samples fulfilled the criteria for the later implemented mechanical tests.

2. A two-component epoxy system (Sikadur-52) was prepared by combining the resin and hardener at a 2:1 weight ratio. The mixture was stirred for 5–7 minutes until it reached a uniform consistency, ensuring efficient curing and excellent mechanical properties.

3. For the hybrid samples, certain additives were incorporated into the epoxy mixture. The first sample was the base sample, while the second sample contained iron powder, and the third sample contained graphite powder, as shown in **Table 3.**

Table 3. The weight ratios of the various sample components.

Material	Sample's Component Weight (g)		
	Sample 1	Sample 2	Sample 3
Kevlar fiber	34	34	34
Graphite	0	0	10
Epoxy	150	150	150
Fe	0	10	10

4. The hand layup method was used to create composite samples. The epoxy mixture was poured into the prepared mold, and then layers of Kevlar 49 fibers (4 cm × 2 cm) were carefully placed. The position of the fibers was controlled using positioning pins to ensure correct orientation.

5. The samples were cured at room temperature (25 °C) for one day under a pressure of 0.1 MPa, and then further cured at 80 °C for 2 hours to enhance cross-linking.

6.After processing, the samples were carefully removed from the molds using dedicated pins to avoid any damage.

7. The treated composite panels were cut into final specimens for testing using a precision water-jet cutter, as shown in **Figure 4,** ensuring dimensional accuracy for mechanical tests.

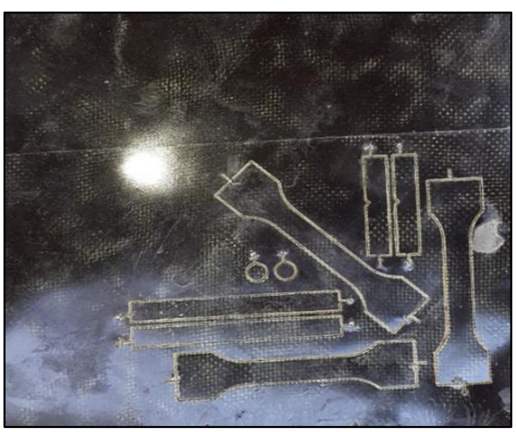

Figure. (4): Samples Preparation using the Water Jet Cutting Technique

8. The edges of the cut specimens were polished with 400-grit sandpaper and then cleaned with isopropyl alcohol.
9. All samples were stored at 23 °C and 50% relative humidity for 48 hours before testing.
10. The composition of each sample was confirmed against the target weight ratios, with microscopic analysis performed to verify sample quality.

Figure 5 Flowchart showing the process of preparing Kevlar-49-reinforced hybrid composite samples, including steps from mold preparation and epoxy mixing to additive incorporation, hand application, curing, cutting, finishing, and conditioning before mechanical testing.

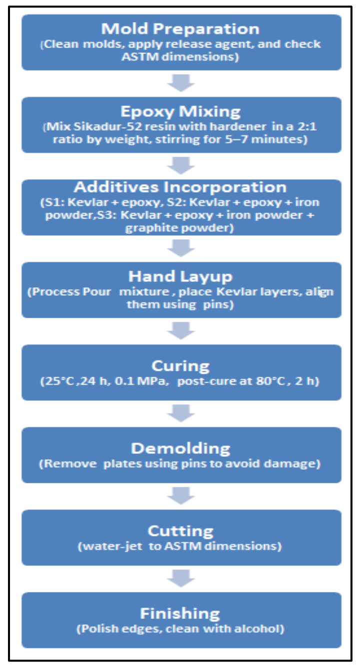

Figure (5): Flowchart of Composite Preparation Process

1.8 Hardness Test

A Vickers hardness tester was used to measure the hardness of the three samples. An indentation was produced using the Vickers hardness tester, which applies a static load through a diamond indenter. The Vickers hardness number was calculated based on the diagonal length of the indentation and the load applied to the indenter. The force applied to the samples was 1 kgf (9.807 N). The diagonal length of the indentation was measured using a microscope.

1.9 Wear test

The wear test was conducted on a Vertical Universal Friction and Wear Testing Machine (MM-W1A model). The load limit was 1 kN, with a sliding rate ranging from 0.1–100 mm/min, and the temperature was controlled from 20 to 100 °C. The wear rate was measured in the range of 10^{-8} to 10^{-5} g/cm. Samples with a 10 mm diameter and 20 mm height were prepared for testing. The test duration was 5 minutes, and the wear rate was determined using g/cm. The weight-loss method was employed to calculate the wear rate by weighing the specimen before and after the experiment, and the difference was used for calculation. Abrasive wear occurs when hard particles such as sand or grit rub against a softer material, resulting in the removal of small surface fragments. The test was performed in a stabilized environment at room temperature (20 °C) and a relative humidity of 50%.

According to Table 4, the wear rates of three wearing samples are presented by the results of the wear test.

Table 4: Comparison of Wear Rates for Different Samples in Wear Test

sample	Wear rate(g/cm)
1	$3.093*10^{-8}$
2	$2.7836*10^{-7}$
3	$2.4743*10^{-7}$

Figure 6 provides a visual representation of the samples used in both the wear and tensile tests, aiding in the understanding of the experimental setup.

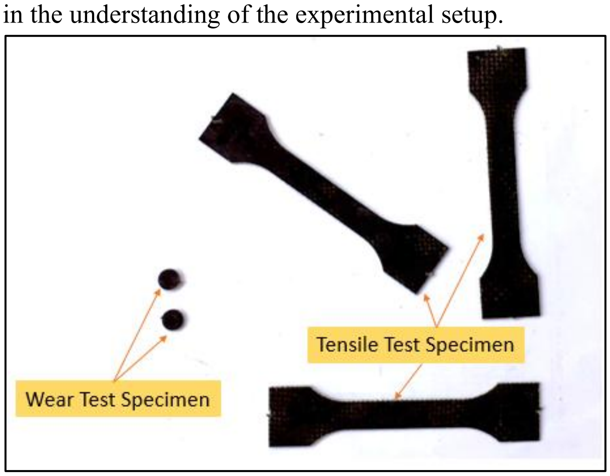

Figure (6) Wear and Tensile Test Specimens for Evaluation

1.10 Tensile test

The tensile test specimens of the three samples (S1, S2, and S3) were fiber-oriented at 90° and 45°. According to ASTM D3039, a standard test method for determining the tensile properties of Kevlar 49 fiber–reinforced composite materials, the samples were cut to evaluate their tensile strength. This test method applies to continuous or discontinuous fiber-reinforced composites in which the laminate is balanced and symmetric with respect to the test direction .The sample size followed the ASTM D3039 dimensions, with a gauge length of 50 mm, a width of 13 mm, and a thickness of 1.6 mm. Figure 7 displays the sample gauge length for the tensile test.

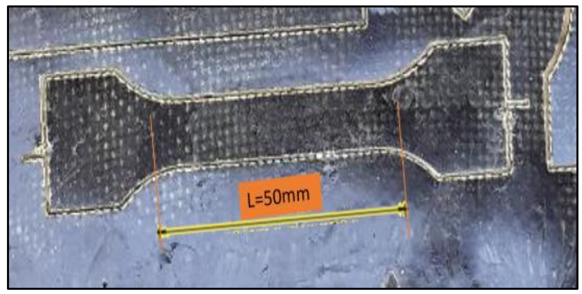

Figure (7) Gauge length of Tensile Test sample

The tensile strength was measured using a universal testing machine (UTM), operated at a crosshead speed of 2 mm/min. It was calculated by dividing the maximum load by the original cross-sectional area of the sample. The tensile test results indicated that the tensile strengths of the three samples at 90° fiber orientation are presented in Table 5.

Table 5: Tensile Strength of Kevlar-49 Reinforced Composites at 90° Fiber Orientation

Sample	Tensile Strength (MPa)
S1	139.42
S2	110.58
S3	105.77

The tensile strengths of the three samples at 45° fiber orientation were as follows in **Table 6:**

Table 6: Tensile Strength of Kevlar-49 Reinforced Composites at 45° Fiber Orientation

Sample	**Tensile Strength (MPa)**
S1	237.5
S2	185
S3	180

2.Results and Discussion

2.1 Hardness Test Results

According to Figure 8, the Vickers hardness values of the three composite samples were measured under a standard load of 1 kgf (9.807 N). Sample 2 is found to be the hardest of the materials measured (70 HV). This enhancement is mainly due to the addition of iron powder in Kevlar–epoxy matrix. Iron particles act as rigid inclusions, limiting local plasticity beneath an indenter and providing resistance to penetration. Moreover, iron also improves load transfer in the matrix, resulting in higher surface hardness.

Sample 1, exclusively from Kevlar fiber and epoxy has a lower hardness value (62HV). Despite the spiking nature of Kevlar fibre for tensile strength and toughness, the unmodified epoxy matrix controls the indentation response and, hence, has lower hardness in the absence of rigid particulate addition.

The sample 3, comprising iron and graphite powders, has a hardness of around 61 HV—graphite-ceramic composites. Even in the presence of iron, graphite decreases hardness due to its lubricating properties and its intrinsically low hardness. Graphite: away from the matrix/ferrite to allow some localized shear and sliding action within the ferrite, thereby opposing the hardening effects of iron. Also, dual fillers may not allow uniform distribution of stress during indentation, resulting in ineffective deformation resistance.

Figure (8) Hardness Comparison of Samples 1, 2, and 3

2.2Wear result

The wear characteristics of the synthesized composites are controlled by the mechanical behavior of the blend components, their uniformity throughout the epoxy matrix, and the major wear mechanisms at the contact surfaces (Figure 9). Sample 1 of Kevlar-49 pure fiber/epoxy had the lowest wear rate. This is because of the high abrasion resistance and toughness of Kevlar fibres, which support the applied load, ultimately protecting the epoxy matrix from direct material removal during sliding contact.

The wear rates of Samples 2 and 3 were greater than that of Sample 1, as iron powder and graphite powders were added. Iron particles may have a strengthening effect on surface hardness, but they would cause local stress concentration and a weak interface bond between the particles and the matrix. In abrasive conditions, these areas will be prone to particle pullout with the "wear" material being worn away. The addition of relatively soft graphite also offers opportunities for micro-scale plowing and matrix smearing to enhance wear despite its lubricant behavior.

The simultaneous presence of iron and graphite in Sample 3 further enhances these effects, with a higher difference in the elastic hardness properties of the fillers relative to the polymer matrix causing issues at the interface, leading to damage and debris formation during sliding. As a result, sample 1 exhibits better wear resistance because its fiber–matrix structure is more uniform and does not contain particulate fillers, which would break the load transfer. These findings suggest that, for the conditions studied, continuous Kevlar-reinforced structure is superior to particulate fillers in withstanding wear.

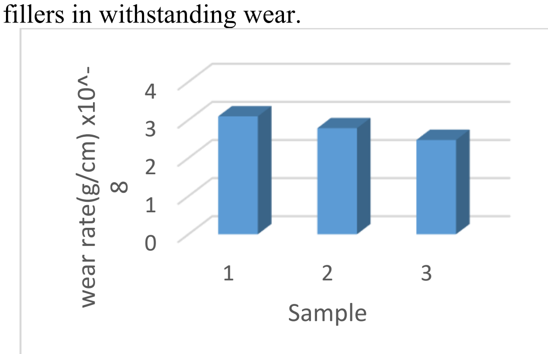

Figure (9) Comparative Analysis of Wear Rates in Kevlar-49 Reinforced Compounds with Different Compositions

2.3 Tensile test at 90° Fiber Orientation.

Tensile tests were performed in accordance with ASTM D3039 on three composite systems with different constituent compositions. The specimens were reinforced with Kevlar-49 fibers and epoxy as the matrix, with iron powder and graphite powder added in Samples 2 and 3 at fixed weight ratios. The corresponding load–extension responses are presented in Figure 10.

Sample 1 (Kevlar/epoxy) showed the best tensile behaviors with a maximum load at 2.9 kN and tensile strength of 139.42 MPa, respectively. This is due to the effective load transfer from the continuous Kevlar fibers to the epoxy matrix, as evidenced by strong bonding at the interface and lack of particulate inclusions that could act as stress raisers. For the axial loading at 90° fiber orientation, the stress is mainly transmitted by the fibers, leading to a high strength and stable extension response.

In contrast, the Maximum load (2.3 kN) and tensile strength (110.58 MPa) of Sample 2, which contains iron powder , were decreased. The weakening of the tensile properties can be physically attributed to the additions of rigid metal particles in the matrix, which could destroy stress continuity and result in stress concentration zones at particle–matrix interfaces. These areas favour early microcrack initiation and prevent efficient stress transfer between the matrix and the fibres.

Sample 3 (a combination of both iron powder and graphite powders) had the least tensile strength (105.77 MPa) as well as the maximum load (2.2 kN). The presence of both metallic and carbonaceous fillers produces microstructural inhomogeneity that may enhance particle agglomerates along with the deteriorated interface bonding. Graphite particles, even though they are beneficial for friction resistance, have poor load-bearing capacity such that under tensile load, interfacial sliding becomes easier with the graphite as a catalyst, resulting in early accumulation of damage and lesser stiffness.

In general, the large changes observed in tensile properties are attributed to interfacial interactions between the fibre-matrix and the fillers. Although the fillers could improve hardness or wear resistance, they are not conducive to tensile performance at these proportions due to changes in stress distribution and failure modes. These results highlight that, under axial tensile loading along the 90 ° fiber direction, the unmodified Kevlar-49/epoxy composite exhibits the best load-carrying capacity and mechanical rigidity.

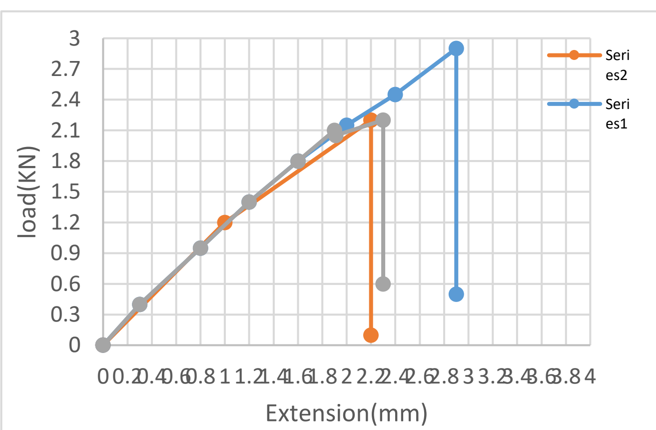

Figure (10) Load and Extension Values for Three Tensile Test Samples at 90° Fibre Orientation.

2.4 Tensile strength

The tensile test results indicate that Sample 1 exhibits the highest tensile strength (139.42 MPa) compared with Sample 2 (110.58 MPa) and Sample 3 (105.77 MPa), as shown in Figure 11. This behavior can be attributed primarily to the absence of particulate fillers and the more effective load transfer between the Kevlar-49 fibers and the epoxy matrix.

In Sample 1, the applied tensile load is efficiently carried by the Kevlar fibers due to their high modulus and tensile strength. At the same time, the epoxy matrix provides uniform stress distribution and effective fiber–matrix interfacial bonding. This results in delayed crack initiation and reduced stress concentration, leading to higher tensile strength.

On the contrary, in Samples 2 and 3, the addition of iron and graphite powder causes new interfaces within the matrix. Such particulate fillers are potential stress concentrators and may cause defects to propagate across the epoxy matrix and thus be detrimental to transfer of stress from the matrix to a fiber reinforcement. In addition, less agglomeration of the particles and weak matrix–filler interface bonding may also contribute to early evolution of microcracks under tensile loading at a 0 II molecular level, resulting in reduced overall strength.

Therefore, although fillers may enhance other properties such as hardness or wear resistance, their presence in the investigated weight fractions adversely affects tensile performance. The results demonstrate that a pure Kevlar-49/epoxy system provides a more favorable stress transfer mechanism and superior tensile behavior under axial loading conditions.

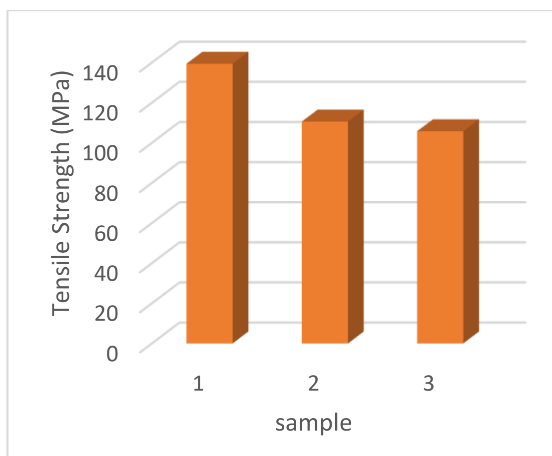

Figure (11) Tensile Strength of Sample 1, Samples 2 and 3

2.5 Tensile test at 45° Fiber Orientation.

Figure 12 shows the tensile strength and elongation at break of the three Kevlar-49-reinforced composites when tested at a fiber orientation angle of 45°, where load is transferred through a combination of fiber tension, matrix shear, as well as fiber–matrix interfacial bonding. In this orientation, mechanical behavior is closely related to the stress-transfer capability and the integrity of the matrix phase.

Sample 1, made of Kevlar fiber and the epoxy only, had a maximum tensile strength (237.5 MPa) and the largest failure strain (5.7%). This can be attributed to the efficient load transfer between Kevlar fibers with epoxy matrix and strong interfacial interaction, so that gradual deformation and stable stress distribution occurred prior to failure, the trends of monotonic increase and sudden reduction in stress.

While samples 2 and 3 had reduced tensile strength compared to their matrix composite (Kevlar/epoxy), sample 3, i.e., Kevlar/epoxy + graphite above iron powders, exhibited the lowest tentative value of approximately ≈180 MPa. The mechanism of stress transfer effectively alters the model by arranging particulate fillers that create local stiffness discontinuities and potential stress concentration zones in the matrix. For the 45° fiber orientation, where substantial shear deformation has been introduced at the matrix–fiber interface, these effects may reduce the bonding at the matrix and fiber interfaces, resulting in debonding or microcrack initiation at an early stage of testing.

The similar mechanisms also manifest in the stress–strain performance of Sample 3. An initial increase, partial decrease and then subsequent rise of the nonmonotonic stress history is prevalent in cumulative damage related to matrix cracking, interfacial debonding between matrix and particles or local load redistribution ahead of final failure. Non-linear mechanical behaviors and damage evolution mechanisms owing to the differences of stiffness between staged constituents and intraction effects have also been reported on engineering composite systems under tensile loadings [30].

Although iron and graphite powders may enhance local stiffness, they reduce overall bending ductility, thereby decreasing the material's capacity to accommodate high shear strains. In general, with a 45° loading direction, the unmodified Kevlar-49/epoxy composite exhibits higher strength and deformability efficiency. The enhancement in shear strength for the specimens containing iron and graphite powders is cancelled, leading to a drop in strain capacity and earlier failure. These results are in good agreement with other studies that emphasize the significant effects of fiber orientation, matrix continuity, and interfacial strength on the off-axis tensile performance of fiber-reinforced composites.[31].

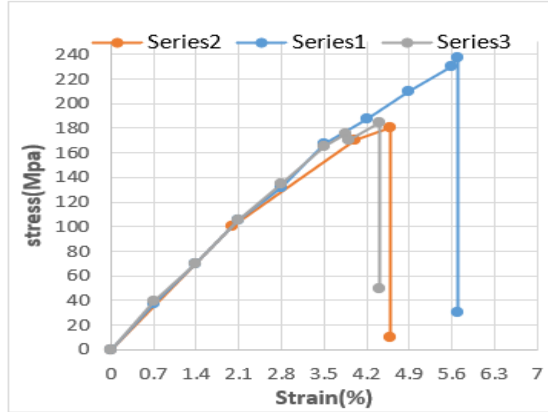

Figure (12) Tensile Strength and Strain Behavior of Kevlar-49 Reinforced Compounds with Different Compositions at 45° Fiber Orientation.

3. Comparison with Previous Studies

The tensile strength value achieved for this Kevlar-49/epoxy composite is compared favorably with reported values for Kevlar-based and hybrid composites in structural applications. Previous investigations of Kevlar–carbon/Kevlar and Kevlar-hybrid laminates have shown that the addition of particulate fillers can improve properties such as hardness, wear resistance, and impact performance, although it usually results in reduced tensile strength due to stress concentration, particle agglomeration, and lower matrix–filler interfacial bonding.

Consistent with these observations, the present results show that tensile properties are not enhanced even in the presence of iron and graphite powders. This result is in line with those commonly reported for hybrid composites, for which particle reinforcements are incorporated into the matrix without rigorously controlling standard procedures such as dispersion, interfacial adhesion, particle size distribution and processing parameters; thus rather than reinforcing (gaining advantage of each reinforcement phase), these phases may act as a stress concentrator and promote microvoids/agglomerates that disrupt macroscopic properties as well weaken load transfer across the fiber–matrix interface. In this respect, the role of nano-materials is of great interest, as nano-scale fillers (e.g., graphene/graphene nanoplatelets, carbon nanotubes, nanoclays, nano-silica or even nano-oxides) can significantly improve performance at relatively low loading levels by reinforcing matrix stiffness, crack-bridging, and energy dissipation—provided that they are properly dispersed into the epoxy network and chemically compatible. Nano-reinforced hybrid systems, when properly engineered, can serve to mitigate interlaminar damage while boosting their fatigue and impact tolerance as well as promoting in some cases, improved tribological behavior elicited by the formation of protective transfer layers; but if dispersion is poor and/or the nano–micro hybrid ratio not balanced, these same mechanisms result in premature cracking and marginal tensile gains. Undoped Kevlar-49/epoxy composite, for its part, does better in a more balanced mechanical behavior, including tensile strength and wearability, than the hybrid formulation. Thus, the material may act as an acceptable baseline material for use in wind turbine blades and a target composite against which to carry out further optimization studies of hybrid composites, in particular nano-enhanced fiber–matrix systems (such as solvent-dispersed, surface-functionalized nanoparticles; hierarchical fiber–particle designs; or graded layups) targeted at providing better interfacial bonding and damage tolerance without sacrificing tensile performance.[32],[38].

Conclusion

The obtained result shows that having iron powder in the Kevlar/epoxy composites (Sample 2: iron powder/Kevlar/epoxy) increases the hardness of material which is 70 Vickers The reinforcement in materials possessing more increased amount of iron particle has excellent loading capacity, and so it has been presented the maximum value while decreasing its abradability and tensile property especially fiber reinforced with graphite particles. The optimal system was found to be sample (pure Kevlar/epoxy) with the best mechanical performance, e.g., higher tensile strength of 139.42 MPa compared to sample (110.58 MPa) and Sample (105.77 MPa), lowest wear rate, and high load carrying capacity of 2.9 KN. The results are listed in Table1. Even though Sample 2 had a higher hardness than Sample 3 (graphite + iron), both the tensile and wear properties of Sample 2 were worse than those of Sample 1. These findings indicate that the combination of additives (iron/graphite) does not enhance overall mechanical properties. Thus, non-modified Kevlar/epoxy composite (Sample 1) is a better candidate to be used for the wind turbine blade due to its well-balanced and superior properties.

In this study, the effectiveness of a hybrid PID–ANN control strategy for PMSM with changing mechanical load conditions and references speed has been confirmed. The suggested strategy combines the simplicity and robustness of traditional PID control with the adaptability and learning capabilities of artificial neural networks to ensure rigid speed control and quick torque response, the controller enabled easy tracking of the reference speed, irrespective of whether the mechanical load was at rest or in motion, the PMSM reaches the reference speed (300 rad/s) at only 0.3s see figure (7).

The future study recommends implementing the proposed system on actual hardware or using HIL for practical performance verification, in addition to developing the neural network and improving real-time learning capabilities, expanding testing to include multiple operating conditions, and conducting deeper stability analysis to ensure higher reliability in industrial applications.

CREDIT AUTHORSHIP CONTRIBUTION STATEMENT

Author contributions M.R and K.A-Writing Original draft, Methodology, Investigation, and Formal analysis. A.A -Main Concept, Data interpretation, and supervision. M.M Writing-Review and editing, Visualization, and Data curation.

DECLARATION OF COMPETING INTEREST

The authors declare that they have no known competing financial interests or personal relationships that could have appeared to influence the work reported in this paper.

ACKNOWLEDGEMENTS

The authors would like to thank the Northern Technical University -Iraq for the logistic support of this work.

References

[1]Abid, H.N., Nayef, U.M., Mutlak, F.AH. et al. Synthesis of Fe3O4 NPs on Porous Silicon for Photoluminescence-Based Humidity Sensor. Plasmonics (2025). https://doi.org/10.1007/s11468-025-03250-7

[2]Raheem, Z., Nayef, U.M., Al-Zubaydi, A.S.J. et al. Laser-Assisted Synthesis of $Mg\text{-}MgO\text{-}Mg_{17}Al_{12}$ Nanoparticles on Porous Silicon for Enhanced Photodetector Performance. Silicon (2025). https://doi.org/10.1007/s12633-025-03393-6

[3]Mustafa, M.M., Ibrahim, M.H., Hussien, A.M. et al. Enhancing the efficiency of hybrid photovoltaic/thermal solar collectors using Al2O3 nanofluids: experimental performance and optimization. Appl Nanosci 15, 51 (2025). https://doi.org/10.1007/s13204-025-03131-9

[4] C. N. Salih, A. H. Taqi, A. A. Aesa, and M. W. Muayad, "High effect of CO 2 laser and gamma irradiation on structural, thermal, and morphological properties of chitosan," Radiation Effects and Defects

in Solids, pp. 1–12, Feb. 2026, doi: 10.1080/10420150.2026.2626688.

[5] Hadi, A.J., Awad, A.T., Nayef, U.M. et al. Influence of Solvent Viscosity on TiO2 Nanoparticle Characteristics and TiO2/n-Si Photodetector Performance via Pulsed Laser Ablation in Liquids. Silicon (2026). https://doi.org/10.1007/s12633-025-03600-4

[6]Mohammad, Omar H., et al. "Machine Learning Algorithms to Enhance PV/T Cooling Performance with Y2O3 Nanofluids." Chemical Engineering Science, vol. 325, 2026, p. 123345, https://doi.org/10.1016/j.ces.2026.123345.

[7] Rashid, M.K., Mohammed, H.j., Hameed, H.M. et al. The effect of titanium dioxide (TiO_2) nanoparticle concentration on the performance of polycrystalline silicon solar cells. J. Umm Al-Qura Univ. Eng.Archit. 16, 1753–1764 (2025). https://doi.org/10.1007/s43995-025-00207-z

[8] Ali, Hussein Hayder Mohammed, Suad H. Danook, and Khadija O. Mohiuddin. "Water Production from Atmospheric Air Using a Solar Water Recuperator by Glass Pyramid Device." Tikrit Journal of Engineering Sciences 32.2 (2025): 1-12.

[9] Özen, H. Gedikli, and B. Öztürk, "Improvement of solid particle erosion resistance of helicopter rotor blade with hybrid composite shield," Engineering Failure Analysis, vol. 121, p. 105175, Dec. 2020, doi: 10.1016/j.engfailanal.2020.105175.

[10] V. V. Maksimović, K. S. Maksimović, M. S. Maksimović, and S. M. Maksimović, "Strength Analysis of Helicopter Tail Rotor Blades Made from Composite Materials," in Lecture notes in networks and systems, 2022, pp. 97–113. doi: 10.1007/978-3-031-19499-3_5.

[11] H. Bansemir and S. Emmerling, "Fatigue Substantiation and Damage Tolerance Evaluation of Fiber Composite Helicopter Components," Applied Vehicle Technology Panel, Feb. 2000, [Online]. Available: https://apps.dtic.mil/dtic/tr/fulltext/u2/p010642.pdf

[12] M. K. F. M. Paudzi, M. F. Abdullah, and A. Ali, "Fatigue Analysis of hybrid composites of Kenaf/Kevlar Fibre reinforced epoxy composites," Jurnal Kejuruteraan, vol. si1, no. 7, pp. 65–70, Nov. 2018, doi: 10.17576/jkukm-2018-si1(7)-08.

[13] Azeez, A., Ali, F.H., Khalaf, I. et al. Enhancing photovoltaic panel efficiency using porous materials under controlled thermal reduction. Heat Mass Transfer 62, 28 (2026). https://doi.org/10.1007/s00231-026-03654-z

[14] Mohammed, W.H., Nafil, R.Q., Nayef, U.M. et al. Effect of 1064-nm Laser Ablation on the Synthesis of Barium Titanate Nanoparticles Deposited on Porous Silicon for Photonic Detector Applications. JOM (2026). https://doi.org/10.1007/s11837-026-08222-8

[15]Awad, Afrah Turki, Abdulelah Hameed Yaseen, and Adnan M. Hussein. "Evaluation of Heat Transfer and Fluid Dynamics across a Backward Facing Step for Mobile Cooling Applications Utilizing CNT Nanofluid in Laminar Conditions." CFD Letters 16 (2024): 140-153.

[16]A. T. Awad and K. J. T. Albazzaz, "NUMERICAL INVESTIGATION OF a HIGH-TEMPERATURE ENERGY STORAGE," MINAR International Journal of Applied Sciences and Technology, vol. 4, no. 4, pp. 133–146, Dec. 2022, doi: 10.47832/2717-8234.13.12.

[17]A. H. Y. A. Daraje, A. Awad, M. Gogazeh, and H. A. M. Khamees, "IMPACT OF MEASUREMENTS TECHNIQUES ON HEAT TRANSFER CHARACTERISTICS IN AIR JET ARRAYS," Journal of Engineering and Sustainable Development, vol. 28, no. 1, pp. 17–34, Jan. 2024, doi: 10.31272/jeasd.28.1.2.

[18] Hussein, A.S., Albarazanchi, A.K.H., Nayef, U.M. et al. Synthesis of NiO, CdO–NiO, and SnO2-NiO nanowires by electrochemical deposition in the anodic aluminum oxide template. J Mater Sci: Mater Electron 37, 420 (2026). https://doi.org/10.1007/s10854-026-16807-x

[19] Bielawski, Radoslaw. "Composite materials in military aviation and selected problems with implementation." Review of the Air Force Academy 1 (2017): 11.

[20] Hamidon, Mohd Hafizal, M. T. H. Sultan, and Ahmad Hamdan Ariffin. "Investigation of mechanical testing on hybrid composite materials." Failure analysis in biocomposites, fibre-reinforced composites and hybrid composites. Woodhead Publishing, 2019. 133-156.

[21] Vasudevan, A., et al. "Experimental and analytical investigation of thermo-mechanical responses of pure epoxy and carbon/Kevlar/S-glass/E-glass/epoxy interply hybrid laminated composites for aerospace applications." International Journal of Polymer Analysis and Characterization 23.7 (2018): 591-605.

[22] Nguyen, Hai, Wael Zatar, and Hiroshi Mutsuyoshi. "Hybrid polymer composites for structural applications." Hybrid Polymer Composite Materials (2017): 35-51.

[23] Hamdan, A., M. T. H. Sultan, and F. Mustapha. "Structural health monitoring of biocomposites, fibre-reinforced composites, and hybrid composite." Structural Health Monitoring of Biocomposites, Fibre-Reinforced Composites and Hybrid Composites. Woodhead Publishing, 2019. 227-242.

[24] Djedid, Toufik, et al. "Mechanical and low-velocity impact properties of sandwich Carbon/Alfa and Kevlar/Alfa fiber-reinforced epoxy for wind turbine blade." Fibers and Polymers (2025): 1-16.

[25] Ram Vishal, Gandham, et al. "Mechanical characterization of carbon/Kevlar hybrid woven 3D

composites." Journal of the Mechanical Behavior of Materials 34.1 (2025): 20250070.

[26] Muhammed, K. Ansal, S. Marimuthu, and Shebin Sharief. "Performance analysis of wind turbine blades using E-Glass fiber and SiO2-Al2O3-TiO2 MMT nanocomposite with AW 106 epoxy." Energy Sources, Part A: Recovery, Utilization, and Environmental Effects 46.1 (2024): 2158-2179.

[27] Hombal, Ranjith R., and H. K. Shivanand. "Fabrication and Characterization of Kenaf and Kevlar Fibre Reinforced Graphene Filled Hybrid Composite Laminates for Engineering Applications." Journal of Mines, Metals & Fuels 73.5 (2025).

[28] Teng, Hanwei, et al. "Carbon fiber composites for large-scale wind turbine blades: Applicability study and comprehensive evaluation in China." Journal of Marine Science and Engineering 11.3 (2023): 624.

[29] Khusiafan, Firas J. "Use of KEVLAR® 49 in aircraft components." Engineering Management Research 7.2 (2018): 14-19.

[30] Pierson, Hugh O. Handbook of carbon, graphite, diamonds and fullerenes: processing, properties and applications. William Andrew, 2012.

[31] Kamal, M.A., Ali, H.H.M. (2025). A review of the effects of key parameters on the performance of horizontal and vertical axis wind turbines. Journal Européen des Systèmes Automatisés, Vol. 58, No. 7, pp. 1453-1461. https://doi.org/10.18280/jesa.580713

[32] K. N. Abed, S. T. Faris, and I. M. Naemah "Effects of Fiber Orientations on Mechanical Properties of a Carbon Fiber Reinforced Composite Material Used in Aircraft Applications "Al-Nahrain Journal for Engineering Sciences, vol. 26, no. 1, pp. 1–6, 2023, doi: 10.29194/NJES.26010001.

[33] P. A. Fareek, A. M. Hussein, and J. A. Yagoob, “Numerical investigation of hybrid nanofluid flow through backward facing step,” AIP Conference Proceedings, vol. 2931, p. 100024, Jan. 2023, doi: 10.1063/5.0180179.

[34] Muayad, M.W., Nayef, U.M., Hadi, A.J. et al. Synthesis of SnO2 Nanoparticles via Laser Ablation for High-Performance Photodetectors. Plasmonics 20, 9191–9202 (2025). https://doi.org/10.1007/s11468-025-02933-5

[35] Y. H. Khadim et al., “Tunable AG@AU Core–Shell nanoparticles synthesized by pulsed laser ablation for dual H 2 S and NO 2 gas sensing on porous silicon,” International Journal of Modern Physics B, Feb. 2026, doi: 10.1142/s0217979226500852.

[36] Rashid, Marwa K., et al. "Integrating Machine Learning and CFD for Enhanced Trailing Edge Serration Design on a NACA 0012 Wind Turbine Blade." International Journal of Thermofluids, vol. 30, 2025, p. 101446, https://doi.org/10.1016/j.ijft.2025.101446.

[37] Hussein, Adnan M., and Afrah T. Awad. "Solar collectors with nanofluid for domestic applications: a review." NTU Journal of Renewable Energy 7.1 (2024): 57-64.

[38] A. Awad, W. Ahmed, and M. Waleed, “Nanotechnology for energy storage,” in Elsevier eBooks, 2021, pp. 495–516. doi: 10.1016/b978-0-12-821346-9.00009-2.